Immersive Virtual Colonoscopy

Seyedkoosha Mirhosseini, Ievgeniia Gutenko, Sushant Ojal, Joseph Marino, and Arie Kaufman, *Fellow, IEEE*

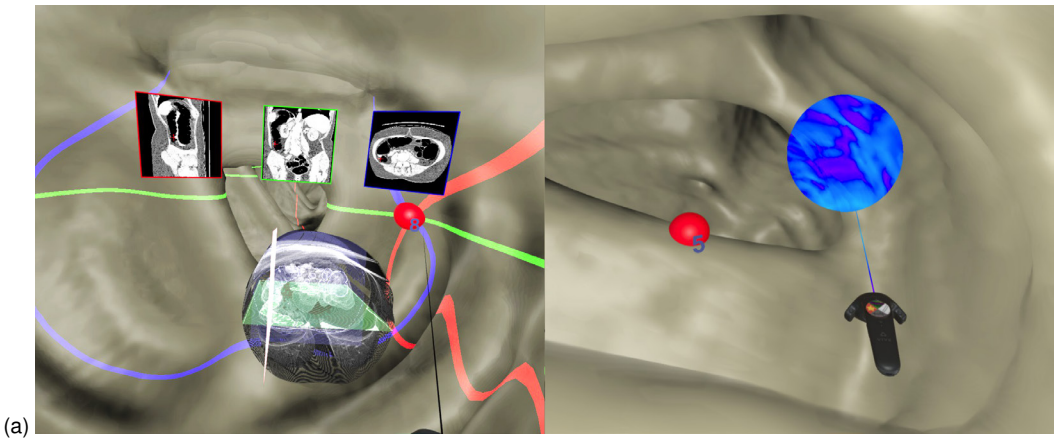

(a) (b)

Fig. 1. Two views of the use of analysis tools inside our immersive virtual colonoscopy (IVC) system. (a) The user has aligned the CT sagittal, coronal, and axial planes with the position of bookmark 8. The planes at bookmark 8, with red, green and blue rectangular borders, respectively, are displayed individually and are also highlighted inside the volume (shown in the circle) by the red, green, and blue planes, respectively; the corresponding areas on the surface are similarly highlighted by red, green, and blue lines. (b) The user is observing the region around bookmark 5 using the electronic biopsy spotlight tool.

Abstract—Virtual colonoscopy (VC) is a non-invasive screening tool for colorectal polyps which employs volume visualization of a colon model reconstructed from a CT scan of the patient's abdomen. We present an immersive analytics system for VC which enhances and improves the traditional desktop VC through the use of VR technologies. Our system, using a head-mounted display (HMD), includes all of the standard VC features, such as the volume rendered endoluminal fly-through, measurement tool, bookmark modes, electronic biopsy, and slice views. The use of VR immersion, stereo, and wider field of view and field of regard has a positive effect on polyp search and analysis tasks in our immersive VC system, a volumetric-based immersive analytics application. Navigation includes enhanced automatic speed and direction controls, based on the user's head orientation, in conjunction with physical navigation for exploration of local proximity. In order to accommodate the resolution and frame rate requirements for HMDs, new rendering techniques have been developed, including mesh-assisted volume raycasting and a novel lighting paradigm. Feedback and further suggestions from expert radiologists show the promise of our system for immersive analysis for VC and encourage new avenues for exploring the use of VR in visualization systems for medical diagnosis.

Index Terms—Immersive Environments, Immersive Analytics, Interaction Design, Volume Rendering, Biomedical Visualization, Colon Cancer Screening, Medical Diagnosis

1 Introduction

Colorectal cancer (CRC) is the third most frequently diagnosed cancer worldwide, and the fourth leading cause of cancer-related mortality with 700,000 deaths per year worldwide. Optical colonoscopy (OC) is an uncomfortable, invasive technique commonly used to screen for CRC. In contrast, virtual colonoscopy (VC) was introduced as a non-invasive, comfortable, fast, and inexpensive procedure for the mass screening of polyps [23], the precursors to CRC. VC reconstructs a 3D colon model from a computed tomography (CT) scan of a patient's abdomen, and a physician virtually navigates through the volume rendered colon model looking for polyps. VC has been shown to be a viable, accurate, and efficient method of screening for colon polyps [46]. The low radiation dosage, recent assignment of CPT codes (e.g., 74263) for insurance reimbursement, lack of side effects from anesthesia, and quick turnaround time for results make VC a prime method for CRC screening.

We present an immersive VC (IVC) system with a tactile tangible interface. Previous work [10, 13, 14, 47, 65] suggests that increasing the field of view (FoV) and field of regard (FoR) can have an impact on experts' performance, enabling them to cover a larger area in less time. However, these works were mostly limited to desktop implementations, and achieved the wider FoV through projections that can cause distortion or unnatural experiences. We have chosen an immersive VR setup for this study to be able to deliver higher FoV and FoR with significantly less distortion of the colon walls compared to the traditional wide-angle view used in desktop VC. The use of VR also allows for better depth cues due to stereoscopy and motion parallax, having the potential for a more accurate recognition of polyps which are typically rounded bumps on the colon wall protruding into the colon lumen.

Previous work [31, 32, 50] also underscores the benefits of a VR environment, such as increased immersion, stereo, wider FoV and FoR, and better perception and understanding of 3D structures in volumetric datasets. Beurden et al. [59] conclude that compared to monocular viewing, stereoscopy helps medical diagnoses by improving spatial understanding and leads to better detection of abnormalities. Since VC relies on spatial understanding and detection of anomalies on the colon mucosa, exploiting the benefits of VR can potentially improve both the accuracy and performance of examination.

• *Seyedkoosha Mirhosseini, Ievgeniia Gutenko, Sushant Ojal, Joseph Marino, and Arie Kaufman are with the Computer Science Department, Stony Brook University, Stony Brook, NY 11794-2424.*
E-mail: {koosha,igutenko,sojal,jmarino,ari}@cs.stonybrook.edu

Manuscript received 10 Sept. 2018; accepted 7 Feb. 2019.
Date of publication 17 Feb. 2019; date of current version 27 Mar. 2019.
For information on obtaining reprints of this article, please send e-mail to: reprints@ieee.org, and reference the Digital Object Identifier below.
Digital Object Identifier no. 10.1109/TVCG.2019.2898763

Several challenges were faced in adapting the desktop VC modality to an IVC system. One such challenge was achieving the requisite rendering speed for the volume rendering of the colon surface. To achieve the necessary frame rate, we use a hybrid volume-mesh lighting pipeline with mesh-assisted empty space skipping during the volumetric raycasting. Another challenge is in mapping the controls of the desktop VC to a suitable modality for immersive VR. We utilize haptic feedback in the interaction tasks, as it has been shown that there is a significant effect of haptic feedback on user performance in 3D object selection tasks [45]. It has also been found that haptic feedback has significant, direct effects on presence in travel-maneuvering tasks [33]. Due to the large FoV, it is also common for the user to not look at the control, even if it is present in the virtual environment, thus further emphasizing the utility of the haptic feedback to reinforce the user's actions. In addition to the controls themselves, the use of tools within the application have also been modified for the immersive VR environment.

The contributions of our paper are as follows:

- An immersive analytics framework for VC, delivering high FoV with significantly less distortion than desktop VC.
- A fast, hybrid volume-mesh lighting pipeline with novel application to real-time volumetric rendering in VR.
- The adaptation of VC tools from a desktop environment to an immersive VR environment, including a virtual spotlight-based electronic biopsy tool for polyp analysis in an immersive setup.
- The mapping of tangible interface interactions to VC and the use of haptic feedback, reducing repetitive stress injury while delivering more natural interactions.
- An informal observational study with domain experts on the usability of various VR tools for IVC.

The paper is organized as follows. In the next section, we introduce the domain background for our application, followed by related work in Section 3. We discuss the requirements for our IVC system in Section 4. Section 5 describes the intended components of IVC and Section 6 describes the rendering technique for implementing and deploying VC in an HMD environment. A discussion of our evaluation, including expert feedback from two VC-trained radiologists, is provided in Section 7, and we conclude the paper in Section 8.

2 Domain Background

In OC, an endoscope is snaked through the colon, from rectum to cecum, and then removed slowly, allowing the physician to view the colon mucosa (the colon interior wall). When performed as a screening examination for colorectal cancer, the main purpose is to examine the colon wall for polyps, the precursors of cancer. If a polyp is found, it is typically measured and removed for biopsy. In general, polyps greater than 5 mm in size are considered significant. Since polyps are slow growing, the test is recommended to be performed every five to ten years for those over the age of fifty.

The OC procedure has a variety of negative indicators, including uncomfortable preparation for the patient, the need for sedation, which in some cases might prove hazardous, the risk of perforating the bowel during the examination, and a small risk of death. Furthermore, due to the geometry of the colon and the abundance of haustral folds and bends throughout, about 25% of the colon mucosa is missed during a typical examination [25]. VC solves these issues by offering a safe and comfortable alternative to OC, and the effectiveness of VC has been demonstrated [46]. CT scans of the patient in two positions, typically supine (lying on the back) and prone (lying on the stomach), are acquired, each taking only a few seconds. Two scans are taken in order to ensure full coverage and complete examination of the colon.

Rather than requiring the full bowel cleansing that is needed for OC, the VC preparation consists of a low residue diet and a barium drink mix, which will tag any leftover materials. After the CT scan, the tagged materials are cleansed electronically and the colon wall reconstructed, taking into account the partial volume effect [62]. As the exam is based solely on CT scans, there is no risk of perforating the colon or death, and there is no need for sedation. In addition, the total time required of the patient is significantly less for VC than for OC, and the cost for VC is considerably less than that of OC.

The only disadvantage of VC over OC is that polyps cannot be physically removed for biopsy if any are found. However, in a typical screening population over the age of fifty, only a small percentage of patients (about 8%) will have polyps; the vast majority of patients will be able to simply wait another five to ten years before having their next exam. For those who are found to have polyps, a follow-up OC will be performed, with the VC results used as guidance to ensure that all polyps are located and removed for biopsy.

The main view of VC is the so-called endoluminal view, which is used for a virtual fly-through inside the colon. For automatic navigation, the virtual camera position is set along the centerline through the colon lumen [7, 60, 61]. Volume rendering with an isosurface transfer function is used to generate imagery of the colon wall. Since some artifacts (e.g., adherent tagged stool) can have a similar appearance as polyps, the physician can switch between the supine and prone views in order to confirm or refute a finding. Various methods for performing automatic registration between the supine and prone models have been well researched [43, 66].

An external view of the colon is provided in the form of a triangular mesh surface. This view allows the user to understand the current position within the endoluminal view inside the colon as related to the colon as a whole. Additionally, bookmarks can be placed on this view and used for immediate access to areas of interest. Since the size of polyps is important, a measurement tool is provided which works in the endoluminal view.

In addition to the typical isosurface volume rendering, a special rendering mode using a translucent transfer function, referred to as an electronic biopsy, is provided. This rendering casts rays into the colon surface, accumulating the density values, and maps higher intensities to red and lower intensities to blue. This electronic biopsy can allow the radiologist to gain some insight into the structure of the tissue within the colon wall or a polyp. This translucent rendering mode has also been used for computer-aided detection (CAD) of colonic polyps [24]. Although its utility for accurately diagnosing malignancy still requires more investigation [37], it remains an important tool which provides a real-time unique view unavailable in an OC.

The original CT slices are still presented within the VC interface for use by the radiologist in interpreting and confirming findings. The original axial CT slices, along with reconstructed sagittal and coronal slices, allow the user to directly inspect the CT imagery in order to make further determinations about a suspicious location identified in the endoluminal view. As radiologists are well trained in understanding these slice views, they are an important part of a final diagnosis.

Since the structure of the colon is similar to that of a cavern which completely surrounds the user, immersive technology is well matched for a VC application. Preliminary work has discussed the applicability of immersive VR techniques for a VC application [39, 40], though our present work is the first complete IVC system to provide all of the required tools for immersive analysis of the colon data with feedback from expert radiologists.

3 Related Work

Immersive analytics has great potential for a variety of applications such as scientific visualization [12]. Previous work has shown that immersion can be helpful for visually analyzing volumetric data [31]. The positive effects of stereo on the understanding of features has also been shown, and it was observed that immersion had the most positive influence on tasks involving visualization and spatially complex search tasks for features in volume datasets [32]. Our current work exploits VR immersion and stereo for their affirmative consequence on search and analysis tasks in a volumetric-based VC application.

Compared to traditional desktop methods of input, immersive interfaces may take advantage of different types of user input. Tangible and touchscreen interfaces have been explored and their performance has been evaluated against a mouse as an input system [4]. It was found that these modalities have no effect on user accuracy, though users were found to perform tasks faster than when using a mouse. In fact,

the tangible interfaces were found to be the fastest, delivering a more intuitive mapping and greater impression of control. Tactile feedback has a significant positive effect on both accuracy and performance of interaction with touchscreen inputs [22]. It has also been highlighted that haptic feedback can improve both immersion and interactivity in VR [44]. Our present work utilizes tangible and tactile interactions for this added benefit.

The issue of combining touch-based navigation with immersive environments for exploring 3D visualization has been addressed [35]. They proposed to use a touch navigation on a mobile device (e.g., a tablet) to interact with rendering, identified a set of interaction modes, and presented a transition workflow between these modes to improve interaction experience while maintaining context. Another problem that has been previously investigated is the issue of touching the void [9], and a possible solution was proposed via the use of transparent surfaces [55]. In contrast, our present work relies on haptic feedback for a number of interactions.

To provide a natural user interface for interacting with a multi-touch wall-mounted display while removing any hindrance to the physical mobility of the user, a "what-you-see-is-what-you-feel" (WYSIWYF) approach [58] has been introduced via the use of a handheld device. For example, a handheld or mobile device can be employed to manipulate a given slicing plane in a direct and intuitive way at any desired position. An interface design and evaluation has been presented that combines tactile and tangible paradigms for 3D visualization to allow 3D data space navigation, cutting plane manipulation, style setting and parametrization, picking seed point placement, spatial selection, and data read-outs [5]. A framework has been developed to address the challenges of providing appropriate overview+detail while navigating through volume data and supporting interactive querying and data exploration in immersive visualization [11]. This approach extends the "worlds in miniature (WIM)" metaphor, simultaneously displaying a large-scale detailed data visualization and an interactive miniature.

There are a number of ways to interact with data in a 3D context, and they can be differentiated between gestures, postures, and quasi-postures [26]. Users can perform such gestures using either a single hand (unimanually) or both hands (bimanually). Bimanual gestures can be fully coordinated or can indicate a more complex coordination between the two hands, which are called symmetric and asymmetric, respectively [19]. Bimanual interaction can be used to select arbitrary surfaces in a 3D environment [27]. A separate study has also been conducted which focused on a variety of techniques and methods, including postures, direct-touch interaction widgets, and bimanual techniques, to support the needs of scientists when exploring datasets spatially [29]. It has been shown that mapping multiple interactions to a single prop (a bar) can be very intuitive for users [28], and we similarly map all user interactions to a single wand device.

The variety of volumetric data interaction techniques can be classified based on user goals and tasks [30], such as selection, picking, measurements, and view adjustment. Interaction selection techniques have been classified into five groups: local, at a distance (ray-based), gaze-directed, voice input, and list selection on volumetric displays [38]. There are a variety of 3D selection techniques, and ray-based methods have been shown to perform better than point-based methods [3]. Our work relies on 3D selection techniques for a number of interactions as described later on. Various types of rays and user feedback have been studied for object selection [18]. That work highlighted the importance of selection and disambiguation stages in object selection. Their Lock Ray results in the shortest selection time with a slightly longer disambiguation time. Our bookmark selection technique is similar to their work, yet relies on haptic feedback during the disambiguation stage for further improvements.

Volumetric data picking refers to choosing a particular point inside the volume, and we use such picking to place locations of bookmarks and of ruler markers for measurements. A method for volumetric data picking has been introduced that provides additional helper views to disambiguate the picking location and allows the user to choose among multiple locations along the ray [42]. They also suggest that 3D picking requires stable hands, and that jittering might influence the accuracy of picking. This finding shows that our tactile interactions are a better choice compared to literal picking in 3D. Additionally, most of our picking is performed on the surface of the volume-rendered colon after cleansing, which makes all of the picking locations visible to the user, and no longer require disambiguation.

Techniques of view or modality adjustment can be performed through a system of modifier widgets [36] or through direct user interaction [42]. Previous work has modified the volumetric view by pointing toward the area of focus [41]. Our work uses a similar metaphor of pointing for the electronic biopsy spotlight.

The problem of performing measurements in a VR environment has been explored, and a set of tools has been proposed for this purpose [17, 20]. A 3D measurement toolkit developed for liver surgery and especially tailored for a VR platform has been discussed [51]. A method for the automatic determination of different-distance based measures (shortest distance, diameters, and wall thickness) has also been presented for segmented anatomic structures [52]. The usability of various 3D measurement techniques has been analyzed for evaluating length, volume, and angles in medical data [49]. We use the distance lines introduced in this work for our polyp measurement tool.

A colonoscopy simulator consisting of 3D visualization and haptic feedback to emulate working with the endoscope has been developed for training [63]. VR and augmented reality have also been used for endoscopy training [6]. VR to assist in closely examining user-defined regions of interest with intuitive zoom by moving one's head forward and backward has also been proposed [21]. Compared to these works for training or limited functionality, our aim is a full system for clinical diagnosis of patient data.

4 System Design Requirements

The goal of this work is to develop an IVC system that improves upon conventional desktop VC systems. To this end, there will be enhancements both to the display (allowing for stereo, more immersion in the virtual colon, and wider FoV and FoR) and to the interaction methods (allowing for less context switching between tasks and improved performance). We seek to preserve the desktop VC tools, which are clinically proven and already familiar to radiologists. We discuss here our requirements and how they have led to our choice of system hardware.

4.1 Display

Many previous papers in desktop VC focus on delivering a higher FoV by using different projection techniques such as fisheye distortion or emulating the physical probe. It has been found that increasing the FoV from 90 degrees to 120 degrees can cut the detection time in half without causing the expert to miss any polyps [65]. However, the same work discusses that going beyond 120 degrees produces unacceptable distortion. The marked distortion created by very large FoVs, such as 360 degrees, has been discussed [10]. Distortion caused by wide FoV visualizations, such as 360 degrees, has been shown to make evaluating polyp size difficult due to stretching and compressing of areas [47]. That work highlighted that a milder 120 degree FoV is preferred, which can decrease the number of fly-throughs needed from 4 to 2 without adding troublesome spatial distortion. It has been suggested that wider angles, such as 140 degrees, can reduce both the number of missed areas and the review time, though the distortion can have a negative impact on visibility of polyp conspicuity [13]. It has been shown that a 140 degree colonoscopy can cover 85% of the surface, and increasing the FoV to 170 degrees reduces missed surfaces modestly [14]. However, all of these techniques add distortion in order to be able to pack a larger FoV to the limited space available on the desktop display. By moving to an immersive setup, we are able to deliver a larger FoR to the user with significantly less distortion than desktop VC.

We have chosen an HMD as the platform for our IVC system. HMDs are a commodity hardware that present an affordable and easy platform on which to deploy immersive visualization. There has been work to determine the appropriate lighting levels in radiology reading rooms [48, 53]. Both works highlight the problem caused by dilation and constriction of the pupil in low light conditions, which causes visual fatigue and reduces diagnostic performance, and the issue of higher

reflection with brighter rooms. HMDs by nature block out surrounding light, providing a suitable reflection-free environment for performing medical reading with constant brightness, and avoiding the problems associated with dilation and constriction of pupils.

4.2 Interaction

The following are the five major interactions within a VC system, with a brief description of their standard method of interaction in traditional desktop VC and how we believe the interaction can be improved and enhanced in an immersive setting using a wand controller:

Navigation. The first task in VC is exploration of the colon surface in search of polyps. On the desktop, the user can fly through the colon along the centerline at a chosen speed, with the camera oriented along this path. In order to deviate from this path and orientation, the user must stop the automatic navigation and use the mouse to manually modify the view, including changing the orientation and moving forward or backwards. In an immersive setting, the user can simply look around within the colon to view the walls, and the navigation is adjusted automatically based on the user's head orientation [40]. We incorporate both automatic navigation along a constrained path and the ability to walk around for local exploration. Since the nonplanar geometry of the colon requires 3 degrees of freedom for navigation, physical navigation of the entire length of the colon is not feasible.

Measurement. Once a suspected polyp is found, measurement of diameter of the abnormality is a basic step in evaluating it. On the desktop, the user must first align the endoluminal view with the polyp using the mouse controls, select the measurement tool from the control panel, clicks an end point on the polyp, and drag a line across the area to be measured. In an immersive setting with a wand controller, this interaction can be simplified to selection using the trackpad and then using the wand as a pointing device to perform the desired measurement, which is shown as an interactable distance line widget [49].

Light tool. The ability to place and move a light source is essential to allow the user to gain a better understanding of the shape of the surface and possible polyp. On the desktop, the user selects the light tool, places a light source, and moves it around with the mouse, limiting control of the light source to a single plane. In an immersive environment, the wand can be used as a simple flashlight metaphor to light the area being aimed at, enabling a natural interface with a much higher degree of freedom compared. It has been previously shown that interfaces with higher DoF interfaces, such as wands, have an intrinsic advantage over 2DoF inputs for fundamental 3D tasks such as light placement [56].

Electronic biopsy. Rendering with a translucent transfer function, called an electronic biopsy, can be helpful to view the interior structure of a polyp [37]. On the desktop, electronic biopsy is initiated in a similar manner to the measurement tool, requiring the user to manually adjust the endoluminal view as required, activate the tool, and place it within the view. In an immersive environment, the wand can be used as a simple flashlight metaphor to provide an electronic biopsy view at the region where it is aimed at, acting as a magic lantern [41].

Bookmarks. When a suspicious location is found, a bookmark can be placed so it can be easily recalled and referred to in the generated report. On the deskotp, the user can visit a bookmark by going to the mesh view, manipulating the mesh as needed to bring the bookmark into view, selecting the bookmark, and returning to the endoluminal view to observe the bookmarked location. In an immersive system, the mesh model can be presented on demand within the current view, and the user can quickly select the appropriate bookmark with the wand.

Slice view. For further confirmation of a finding, the radiologist will examine the original 2D CT slice data. On the desktop, slice views are always present, but in small periphery windows; a larger version can be viewed by swapping with the endoluminal view in the main window. On an immersive system, the slice views can be displayed directly within the endoluminal view, making interaction and comparison with them more immediate since they are both present in the user's FoV.

5 System Components

Our IVC system was designed to provide equivalent functionality to the desktop VC, but with the following two enhancements:

1. Full immersion via VR within the virtual colon model through the use of an HMD.
2. Enhanced automatic navigation which flies along the centerline and also modulates speed based on the user's head orientation.

Compared to a typical desktop VC system, a fully immersive VR environment allows for better depth cues due to stereoscopy and motion parallax with head tracking, which have been shown to be beneficial for object understanding and manipulation [31, 32]. The stereoscopy can function as a second cue in highlighting surface bumps. This can deliver to the user better spatial perception, yielding a better understanding of surface placement and relative position of irregularities. This can be advantageous not only in the primary endoluminal view but also to allow users to observe depth changes when using the electronic biopsy mode. Integrating the visualizations within a single view enables users to move freely from one rendering mode to another without losing the frame of reference for their location within the colon.

While the desktop VC requires users to navigate using a mouse to control their view direction, a VR system allows users to freely look around the colon lumen. Since controls are no longer needed to manage the virtual camera orientation, removing the need to control the fly-through speed and direction can also be advantageous.

The use of the mouse-centered interface on the desktop combined with a typical menu setup and keyboard shortcuts, requires the user to constantly shift attention and perform repetitive motions such as mouse clicking when moving between various modes. Carpal tunnel syndrome caused by repeated clicking has been highlighted [8], and solutions such as split keyboards, head mounted headsets, taking frequent breaks, and performing wrist exercises have been suggested [54].

In our system, we use a simple wand device, the HTC Vive controller, for user input. A touchpad is located on top of the hand grip and can be used for swiping, gestures, and selection, while a trigger button is located on the underside of the hand grip. Rather than using the mouse to enter a menu away from the main view, our single controller paradigm allows the user to easily switch between modes by simply performing a gesture on the touchpad or pressing the associated button for that tool. In this way, the tools are immediately available at their finger tips at any given time. Furthermore, our system is simplified to the point that there are no menus and all interactions are only one touch away, using two trigger buttons and gestures on a touchpad.

In our system, all of the visualizations are merged into the same space. However, since the measurement, bookmarks, and biopsy widgets have a spatial aspect to them, they can be placed and used in the same virtual space of the colon. At the same time, due to having a tangible controller with 6 DoF tracking, the user has a wide range of freedom while interacting with the scene. This enables more natural interactions, and the additional freedom can be used to choose different tools from the same one-handed controller. The difference from a mouse interface becomes wider when we realize that in VR we can remap the surface of the controller to show interactions that are suitable to the context that the user is in. For example, a delete operation can be displayed on the virtual controller when pointing toward a bookmark.

5.1 Data Processing

The data pre-processing pipeline is shown in Figure 2. Given the input CT data as raw DICOM files, the colon is first electronically cleansed [62] and segmented [24]. This segmentation is used to then extract a triangular mesh model [16] and a centerline [7]. The centerline, which is used for the automatic navigation, is smoothed to reduce camera jitter during the fly-through. Additionally, the camera view and up vectors are produced to ensure minimum camera roll, and the B-spline is interpolated and sampled to ensure a constant pace along the path. This sampled centerline, along with the original CT data and the triangular mesh, are then used to create the final volume rendered endoluminal view. Volumetric rendering is the *de facto* standard for detailed visualization of the CT colon surface data in VC, and also allows for a translucent electronic biopsy view.

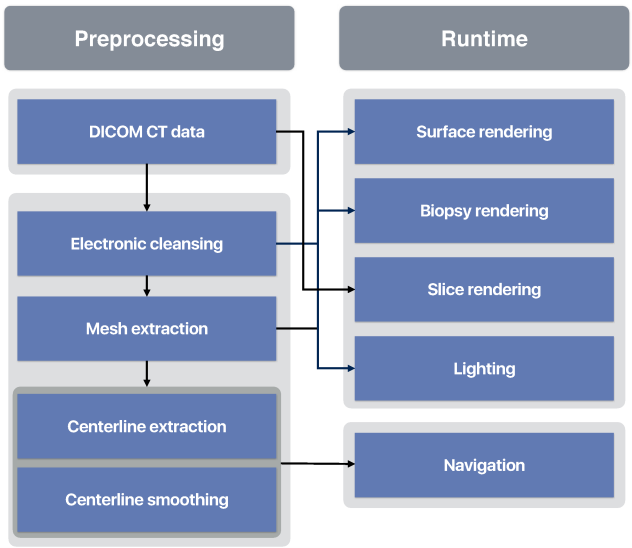

Fig. 2. Pre-processing pipeline. Our system pre-processes the DICOM CT data to produce the cleansed volume, internal isosurface mesh, and centerline. Camera orientation is evaluated by fitting a B-Spline constraining the camera roll. Except for the CT slice views, the extracted mesh is used in addition to the volume in every aspect of rendering.

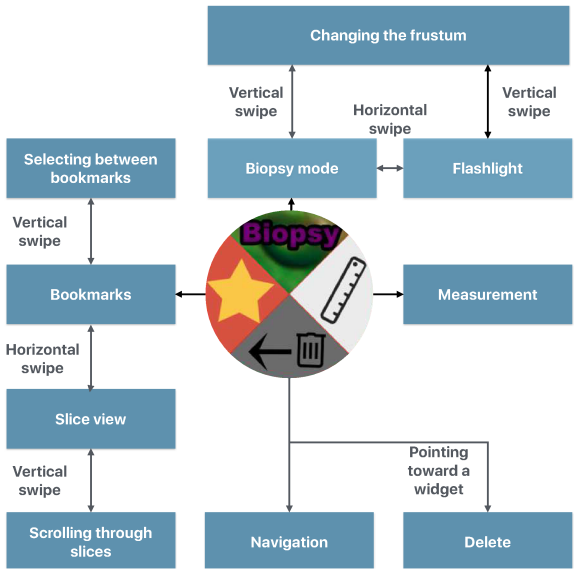

Fig. 3. Interaction state machine. The touchpad is divided into four sections, each corresponding to a separate tool. The circular image is presented in the VR environment on top of the virtual wand. In each mode, the user can modify parameters, such as frustum or current slice, by performing touch gestures or pointing toward a different area. Haptic feedback is also provided corresponding to the touch gestures.

5.2 Interaction

Throughout our system we maintain a uniform approach for dealing with interactions and responses, by mapping swipe up and down to move between different slices, targets, or different frustum sizes. We map the grip button to grabbing and rotating items such as the mesh and volumetric view. We map the trigger button to selecting or placing widgets on the visualization. We swipe left to right to change between different modalities on a visualization. The interaction state machine for our IVC system is shown in Figure 3. Our system was designed around unimanual interaction, which is sufficient to cover all needed use cases without the need for added complexity. Additionally, this frees the secondary hand to be used with other gadgets, such as a microphone, in future clinical settings. While some of the interactions proposed here are also applicable in traditional 2D desktops, due to the 6 degrees of freedom input system that is required they have a higher synergy with immersive 3D displays such as HMDs.

5.3 Fly-through

The main view of any VC system is the virtual fly-through the colon lumen, which allows for inspection of the colon walls. During this fly-through, the virtual camera will typically follow a predefined centerline path through the colon. To relieve the user of the burden of navigation control, we utilize a method of automatic speed and direction control to dynamically adjust both the fly-through speed and direction based on the user's head orientation [40]. In brief, as the user's head orientation becomes further off-axis with regards to the navigation path, the speed of the fly-through will decrease and can stop when the user turns 90 degrees. When the user returns to an on-axis view along the path, the speed will return to the normal fly-through speed. If the user turns a full 180 degrees around, the direction of the fly-through will reverse. This automatic navigation frees the experts from having to focus on navigation and positioning. Our previous work evaluated this navigation method in a very similar application and found no impact on system usability or mental load, while most participants ranked the automatic control as one of their favorite navigation methods [40]. Additionally, navigation based on physical movement is infeasible due to the need to traverse the non-planar 3D geometry of the colon.

5.4 Measurement Mode

In the desktop VC, the user must move the mouse to draw a virtual line with the cursor over the endoluminal view. In our IVC system, the measurement widgets are used to perform the task. The user places these widgets by simply pointing and pressing the trigger toward the surface of the colon with the controller, and each endpoint of a measurement can be moved later by dragging and dropping over the isosurface layer. Compared to the desktop system, our gesture-based method is more natural, due to the use of the user's hand as a pointer for dragging and dropping the measurement endpoints. Moreover, the use of VR decouples the measurement tool from the camera, allowing users to freely manipulate the camera position by simply moving their head. This ease of control enables experts to better observe depth cues as to where the endpoints have been placed. Additionally, users can modify previously added measurements by simply pointing toward an endpoint and moving it along the surface of the colon. Due to this freedom of orientation, it is necessary to assure that the text is always rendered readable in an upright direction.

One of the challenges to correctly render the measurement was to render at the right depth to not interfere with the user's depth perception, while not being crowded by various parts of the colon during navigation. To achieve this, the measurement widget is always rendered at the same depth as the colon surface. However, it is at all times maintained on top. To make sure that the text of the measurements are always available but not moving with the camera movement, textual information is set to face the centerline of the colon (i.e., the camera path). However, the up vector of the text is set to be parallel with the up vector of the user's physical space while placing the measurement. Due to the limited and smooth change in camera orientation (specifically roll) through the fly-through, the up vectors change very slowly throughout the colon, enabling users to read a measurement made at a close position without having to rotate their heads. Moreover, to make sure the measurements are always distinguishable from each other, each measurement is given a new color. These colors are generated using a ColorBrewer diverging color scheme, which has been chosen to be safe for colorblindness (see Figure 4(c)). Since radiologists will tend to place multiple measurements near each other to measure height, width, and depth of a polyp, the diverging color scheme assures that such a sequence of widgets would have different colors and be easy to differentiate.

5.5 Bookmark Mode

In the desktop VC, the user must change between view windows in order to place or utilize previously placed bookmarks. In our IVC system, the bookmarking mode is activated by a selection on the controller touchpad. Pressing the trigger on the controller triggers the bookmark placement. The location of the bookmark is determined by

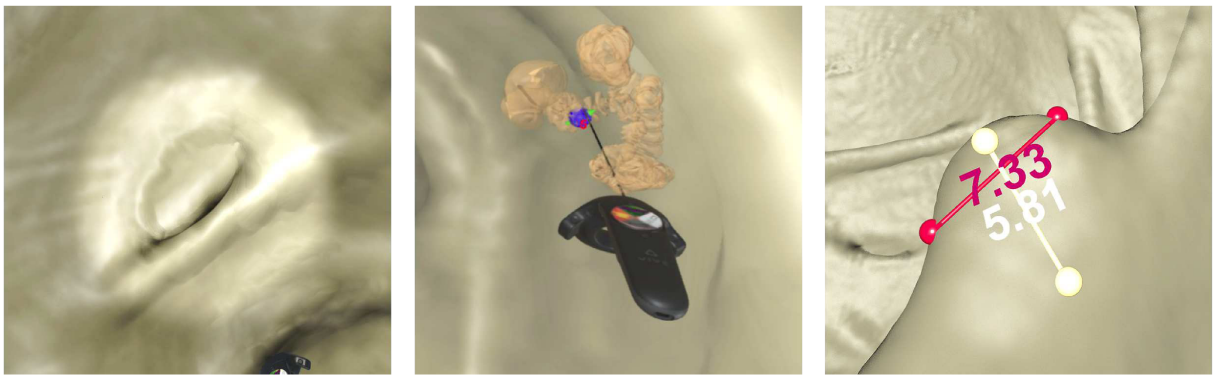

(a) (b) (c)

Fig. 4. Three views inside our IVC system. (a) The flashlight highlighting a cavity (distinguishing it from a convex shape). (b) The user selects a bookmark on the small 3D external view model of the colon near the current position in the colon to jump to. (c) Two measurement widgets are placed on the colon surface to evaluate the size of a region of interest.

casting a ray from the virtual controller to the intersection with the colon wall. The ray is shown as a thick line connecting the two points, thus providing visual feedback on the exact location of the bookmark. The user can later jump to a bookmarked location by selecting it from a small external view 3D model of the colon (see Figure 4(b)). This WIM model is only shown during bookmarking mode, and can be interacted with and rotated using the wand. The small model of the colon is rendered transparently, enabling the user to easily see various bookmarks alongside the path. When the user points the wand toward one of these bookmarks, they are presented with the corresponding label. If multiple bookmarks are placed close together, the user can navigate between them by swiping up and down along the touchpad.

Every time a new bookmark is created, the user is presented with a new sequentially generated label and receives haptic feedback. The device is running at 11ms per frame (90 Hz), and the vibration intensity of this haptic feedback is set to 2000 microseconds within a frame, which is the medium level producible by the device. The user can remove a previously placed bookmark by pointing towards it; the back button on the touchpad is replaced with a delete button, which will remove the bookmark. This erasure interaction is shared between both the bookmark and the measurement widgets, enabling the user to easily remove previously placed widgets.

5.6 Flashlight Tool

The flashlight tool allows the user to shine an extra beam of light where desired, allowing for additional illumination and to help determine whether regions are concave or convex (see Figure 4(a)). In the traditional desktop VC, the user must toggle on the additional light source, and then use the mouse to position it within the 3D scene. For our IVC system, we redefine this tool as a simple pointing gesture using the VR wand controller. The tool is easily toggled through the use of the touchpad controller and the view is positioned within the scene as if the user is naturally holding a flashlight. The extra light is presented as a circle, and the user can adjust its diameter by scrolling up and down on the controller's touchpad. Moreover, the user receives haptic feedback for every 2-degree change in frustum of the flashlight beam. Since VC relies on volumetric rendering for visualization of the internal surface of the colon, this user controlled light also emphasizes the need for a real-time volume rendering system with dynamic lighting and shadows.

5.7 Electronic Biopsy Mode

The electronic biopsy mode performs a rendering on a portion of the surface to accumulate values within the colon wall (as opposed to the isosurface rendering that is typically used). In the traditional desktop VC, the user must use the mouse to first stop the camera motion, toggle the electronic biopsy mode, and then position the biopsy window within the endoluminal view. These steps require the user's focus to change between different views. As with the flashlight tool, we redefine this mode as a simple pointing gesture using the VR controller. To match the flashlight paradigm, the electronic biopsy window is also a circle, and the user can adjust it as previously described.

5.8 Slice Viewing

While in bookmarking mode, users can swipe over the touchpad to switch between an overall mesh view of the colon or a volumetrically rendered model of the colon with the three intersecting cutting planes (see Figure 1(a)). This volumetric view shows the user the position of all the three cutting planes, which the user can interact with and move each of them across the volume. Experts can rotate the volumetric data the same way as in the bookmark view. There are also three cutting planes visualized over the volume which are also visualized separately above the volume as individual images (see Figure 1(a)). Users can navigate through the slices individually by easily pointing toward them and moving their finger across the touchpad, and there is haptic feedback for each layer passed. Users can also move the slices by pointing toward one, two, or all three inside the volume, and can even move multiple slices at the same time. Visualization of the surrounding area is updated to show the cutting planes over the volume around the user (red for X, blue for Y, and green for Z). Users can also bring a plane to their point of interest over the surface by simply pointing toward the surface and pressing the trigger button.

6 Rendering

Our IVC system contains three light sources: a directional light from the user's head (which acts as a headlight), a point light following the navigation, and a spotlight following the wand. The wand spotlight is significantly weaker and with a short range, and is provided for when the user is close to the surface it can be used to more easily observe the shape of the surface. When the user is far from the surface, the spotlight has no effect on the rendering. The point light source is provided since the navigational position is locked along the fly-through path and is separate from the user's head position in the world.

Throughout the system, volume rendering is used for both the electronic biopsy view and for rendering the interior surface of the colon, the mucosa. An internal mesh of the colon is used to assist and accelerate the volume rendering and illumination passes.

6.1 Mesh-assisted Volume Rendering

Volume rendering and VR are both very demanding tasks on the GPU. In our evaluation of normal isosurface volume rendering, its performance fell short of attaining the required rendering frequency for an interactive VR experience, taking more than 100ms per frame. Since the colon lumen is cleansed (either physically or electronically), this empty interior is mapped to full transparency by the volume rendering transfer function and thus has no visual impact on the final rendered imagery. Due to this, we can perform empty space skipping [34] to improve the rendering performance. The empty space is skipped by performing surface-assisted raycasting using the extracted mesh isosurface of the colon as the starting position of the rays [23, 64]. Performing

this empty space skipping greatly reduces the number of points which must be sampled in the volume. This is especially true in rendering an isosurface such as the colon wall, where the ray will be terminated shortly after hitting the tissue density voxels. For medical visualization, volumetric rendering of the final imagery is the *de facto* standard, and thus rendering the mesh directly is not appropriate for our application.

Due to the flexible shader model of newer GPUs, we can perform raycasting during the rasterization phase. After the mesh location has been rasterized, the mesh surface position in world space is transformed to the corresponding location in the local space of the volume data. This fragment location in volume space is used to create an origin and direction for each ray used in the raycasting process. Since the mesh is only a discrete approximation of the colon isosurface, we start the raycasting a few steps back from the surface in order to ensure a smooth rendering through the volume as the voxels transition from air to tissue.

6.2 Hybrid Mesh-Volume Lighting Model

Lighting plays an important role in observing surface shapes, since real-time shadows and dynamic lights help as visual cues for better perception within the colon. However, calculating light attenuation and shadows can be very expensive as it requires ray-casting toward each one of the light sources when rendering each sampling point. We propose here a novel technique which uses the surface mesh to perform space skipping for the lighting phase.

The mesh-assisted empty space skipping is extended from the camera position to also be used for each of the light source positions. In Figure 5, the empty space is skipped from the camera/light until the mesh surface (shown in yellow) is reached. Starting from this mesh surface, the ray is then cast into the volume (represented by the thick brown lines), and a general lighting model including spherical harmonics [57] and the ambient term is used. Along the ray in the volume, the lighting equation for each sample is as follows:

$$\begin{aligned} C_V &= \text{spherical harmonic + ambient} \\ \alpha_V &= impact(|\nabla V|) \end{aligned} \tag{1}$$

C_V is the color for the sampled voxel, α_V is the alpha value for the sampled voxel, and $|\nabla V|$ is the magnitude of the gradient of the sampled voxel. For our current implementation, the *impact* function is a simple linear function, though various transfer functions can be used instead. In our system, this allows for overlaying several translucent isosurfaces to achieve a smooth air-tissue interface.

The samples along the ray are combined by summation as follows:

$$C = C + C_V * \alpha_V \tag{2}$$

where C is the accumulated color along the ray, C_V is the color at the sampled voxel, and α_V is the alpha value at the sampled voxel. This can be changed to an exponential sum, but for our application we prefer isosurfaces closer to the camera.

When sampling from the volume toward the light, the ray will proceed up to a maximum fixed distance from the sampled voxel, which was defined empirically to be the maximum distance between the mesh surface and the volumetric isosurface of interest. This distance threshold is the maximum number of samples attempted before terminating the ray. Allowing for the possibility of an error of two voxels between the volume and the extracted surface, the further away the ray is from being perpendicular to the surface, the greater the distance that may need to be traversed before reaching the surface. Using a maximum distance of 20 voxels guarantees exact lighting for any ray within 84 degrees of the surface normal ($\arccos(1/20)$). Rendering performance can be improved by reducing this threshold. A diagram view of this is given in Figure 5. The ray is terminated when it either hits the mesh surface which was seen by the light source, or reaches this maximum distance threshold. Due to this behavior, regions of the volume further away will not be taken into account when calculating the light attenuation model. As shown in Figure 6, the light source can be blocked by further regions of the surface. However, some areas that were blocked by the mesh surface are not necessarily blocked by the actual volumetric surface, as shown by the vertical line at the top of the rightmost peak in Figure 6.

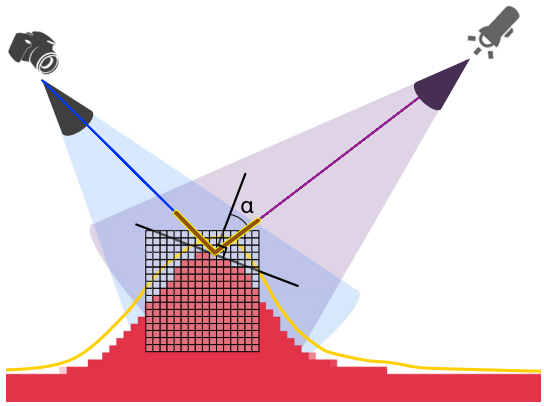

Fig. 5. The rays traversed in traditional raycasting are shown using a blue line from the camera to the observed point and a purple line to the light source. The thick brown lines correspond to the areas raycasted in our pipeline after empty space skipping. The blue and purple regions correspond to the frustums of the camera and light source, respectively, which are rasterized to produce the image and shadow maps. The yellow line corresponds to the surface of the mesh, and the red area corresponds to the tissue region of the volume.The ray toward the light is sampled for 3 voxels, before surpassing the mesh surface. The discrete grid of voxels is represented here by the grid overlay and the stepped surface for illustrative purposes.

For each light source L, the sampled voxels along the ray path are rendered in a similar manner but using the following light equation:

$$L_M = T_s(cam, L) + D_s(cam, L) \tag{3}$$

where D_s is the diffuse component and T_s is the specular component, which can be calculated as

$$D_s(cam, L) = \mu \times C_L \times C_V \times max(0, \overrightarrow{n} \cdot \overrightarrow{l}) \tag{4}$$

$$T_s(cam, L) = \mu \times C_L \times C_V \times max(0, \overrightarrow{n} \cdot \hat{r})^S \tag{5}$$

where $\overrightarrow{r} = \overrightarrow{v} + \overrightarrow{l}$, μ is the light attenuation, C_L is the color of the light, C_V is the color of the sampled voxel, $\overrightarrow{n}$ is the normal direction, $\overrightarrow{l}$ is the light direction, $\overrightarrow{v}$ is the vector from the point to the viewer, and S is the shininess coefficient.

The received light intensity i_v at a sampled voxel is given by

$$i_V = \frac{I_k}{d^2} \times \mu_T \tag{6}$$

$$\mu_T = \mu_V \times \mu_M \tag{7}$$

where μ_T is the transferred attenuation, I_k is the intensity of the light source, and d^2 is the squared distance from the light source to the sampled point. The transferred attenuation μ_T is the product of the attenuation in the volume μ_V and the attenuation in the mesh μ_M.

6.3 Graphics Pipeline Implementation

We map the volume rendering to a forward rendering path. In forward rendering, the scene is rendered from the perspective of each light source, producing a shadow map for each light. The shadow map is the depth map of the camera rendered from the perspective of the light source. Later, the scene is rendered from the perspective of the camera to find the previously rendered sections, along with an extra pass for each main light source. We map volume rendering to this scenario, which results in three different passes: shadow casting, object rendering, and per-source lighting.

Shadow Casting We have implemented a shadow casting renderer that renders the volume, but operates as a cutout shader. For each fragment of the mesh that does not have the volume behind it, the shader discards that fragment, resulting in no shadow being cast from that point. For example, in Figure 6, when the extracted mesh is viewed horizontally, there is no volume behind the mesh and thus it should be discarded from the shadow casting process. Based on the location and orientation of the purple light source, the emitted light for this source would cause the object to cast a shadow on the surface behind it.

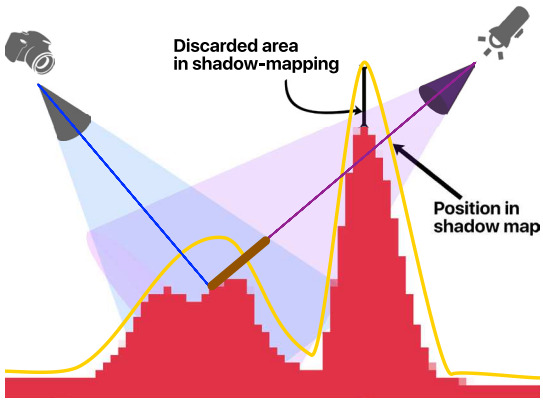

Fig. 6. The light from the light source is obstructed by a section of the volume, resulting in the shadow map having a shorter depth than our sampling threshold. The sampling threshold toward the light source is highlighted by the thick brown line. The top of the rightmost peak illustrates how the mesh surface can block the light, while the actual underlying volume data does not. The yellow line corresponds to the mesh surface, and the red area corresponds to the volume tissue region.

Object Rendering The volume is rendered once for general lighting, including the ambient term and the spherical harmonic lighting. To make sure that only the parts of volume that are close to the camera are being rendered, this pass performs z-testing and also writes updates to the z-buffer. This renderer also works in a cutout fashion, which discards fragments that do not have any volume behind them, to avoid having ghost surfaces and shadows while rendering.

Per-Source Lighting For each light source, the fragments are rendered again, casting rays, and each voxel along the ray path is rendered in a similar manner. This pass does not update the z-buffer, but performs equal z-testing to make sure all fragments that were discarded in the object rendering path are discarded again. This is accomplished before performing any raycasting, in order to increase rendering performance. Our system looks for the position of the sample in the shadow map, reading the shadow map depth. If the number of samples required in the volume to reach the shadow map is above the threshold, then the surface is obstructed. If not, then the volume is sampled toward the light source until the point in the light map is reached. The density of the voxels along the path are summed to calculate the light absorption throughout the volume. When the point in the shadow map is reached, the light value of this shadow map is multiplied by 1-absorption throughout the volume to determine how much of the illumination from the light position has reached our voxel.

This enables our volume renderer to integrate with the lighting models present in the state of the art game engines, rendering multiple light sources over the volume without a significant performance penalty. With a few hints, our system can also integrate with the pre-rendered illumination pipeline of these game engines, and use the baked directional light maps during runtime for specular lighting of the volume.

We evaluated our system against volume rendering without mesh assisted empty space skipping on an NVIDIA 980 GPU. In contrast to our IVC system, our test scene (see supplementary video) contained two light sources, a directional light moving with the camera and a spotlight, to highlight the shadowing results. Compared to the final IVC system, the point light moving with the navigation was removed, the directional light was weaker, and the spotlight was strengthened. A normal volume renderer took more than 100ms during the most demanding part of the fly-through. Our system was capable of rendering the same scene in 25ms and produced an identical result. Throughout the fly-through, we observed an average speed-up of $3\times$. Due to this increased performance, our system was able to maintain an average rendering frequency of 40 frames per second throughout the entire fly-through.

6.4 Implementation Details

Our system was developed in Unity, utilizing the forward rendering pipeline, which is critical for both volume rendering and VR. This enables techniques such as multisample anti-aliasing to improve VR quality, and simplifies the rendering of semi-transparent objects, such as volumes and overlays without the need for peeling. We used an automatic fly-through asset from the Unity asset store [1], and relied on Unity to produce light maps and the rendering system. To correct for volume-mesh intersection in the volumetric view, we used the depth buffer to skip the areas in the volume occluded with widget meshes.

7 Evaluation

We have evaluated our IVC system using real CT colon data from the publicly available National Biomedical Imaging Archive (NBIA) Image and Clinical Data Repository[1] provided by the National Institute of Health (NIH). We performed electronic colon cleansing incorporating the partial volume effect [62], segmentation with topological simplification [24], extraction of a skeleton centerline through the colon lumen [7], and reconstruction of the colon surface as a triangular mesh via surface nets [16] on the original CT images in a pre-processing step. Though the size and resolution of each CT volume varies between clinical datasets, the general data size is approximately $512\times512\times450$ voxels with a voxel resolution of approximately $0.7\times0.7\times1.0$ mm.

7.1 Experimental Setup

We have performed an observational study with two domain experts, radiologists Dr. Matthew Barish (M.B.) and Dr. Kevin Baker (K.B.) from the Stony Brook University Hospital. Both of the radiologists have worked with traditional desktop VC systems, including Viatronix, Vital Images, and Philips, which are FDA-approved for clinical use for colorectal cancer screening. M.B. is a pioneer and trainer of the VC system and is highly familiar with the features of the traditional system and their evolution. Both users were introduced to the IVC system here for the first time, and did not have any prior VR experience.

Our evaluation was performed on a machine with 8GB of RAM, an NVidia 1080 GPU, Intel Xeon 2600 Processor, and an HTC Vive HMD, controllers, and tracking system. We utilize the touchpad surface of the HTC Vive controllers as a 6 degrees of freedom tracked tangible interface. Participants were first shown a 10 minute overview and introduction to the IVC system, the location of the buttons on the controller, and the interaction methods for the navigation modes. Each participant then took turns to navigate the colon dataset using a fly-through mode for another 5 minutes. During this initial exploratory navigation, participants were been given detailed instructions on how to use the features. They were given additional time to investigate the dataset, and to evaluate the internal surface of the colon.

7.2 Expert Feedback and Discussion

The participants initially expressed common feedback on the experience in general. Overall, they were excited about the option to use the system either sitting or standing up. While previous studies have shown that radiologists' reading performance increases while walking (almost jogging) on a treadmill [15], the space requirements for this are often constraining in a clinical setting. Additionally, the spatial complexity of mapping a colon dataset to a path could be confusing.

The participants enjoyed the use of the tangible controller, and noted that it is more convenient than the traditional mouse-based controls, which they have found to be exhausting and a cause of repetitive stress injury. This point was highlighted specifically, as one of our experts was suffering from persistent shoulder pain, which was also mentioned by the other expert. While this effect was not evaluated in the study due to the short study time, it was highlighted by the experts that the freedom of hand motion would remove this problem. Haptic feedback on features such as slice scrolling was found to be very useful. The experts have asked for additional haptic feedback to be added to indicate the boundaries of the colon when these boundaries are outside the FoV (e.g., when backing up).

K.B. found the initial fly-through nauseating, but noted that this is something one could get used to with experience. However, this can be an initial constraint on performance. The experts also addressed the

[1] https://wiki.nci.nih.gov/display/CIP/Virtual+Colonoscopy

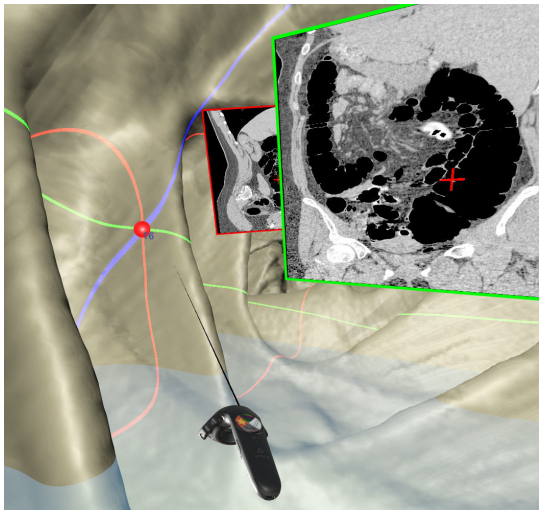

Fig. 7. View of the system after modifications following expert user feedback. The crosshair corresponds to the location of bookmark 16, which the user has interacted with to magnify the coronal view. Additionally, a virtual "floor" was added as a transparent blue plane, to make the immersive experience more intuitive by adding a perception of a floor which corresponds to its physical counterpart as felt by the operator.

importance of the wider FoV compared to the traditional VC system, noting that a further study may be conducted to evaluate how much of the colon surface area has been missed. In a traditional desktop VC, one would typically need to navigate back (retrograde from the cecum to the rectum) to investigate missed areas, while in our immersive system the user can simply look around to observe the missed areas. Hence, greater coverage could indicate potential time savings for the diagnostic procedure. Additionally, they commented that the fly-through in our IVC felt shorter than in the typical VC. A future study is needed to evaluate whether this time difference was real or only perceived (perhaps due to the novelty of the system).

7.2.1 Navigation Fly-through

Our system uses the user's head orientation to manipulate the camera along the constrained path for navigation and direction control. When the user investigates an area outside of the path, the camera slows down. In a traditional VC system, the camera moves along the path with a constant speed and with several speed presets. In IVC, the user was able to reverse the fly-through direction by using either automatic direction control based on head orientation or by pressing the menu button on the wand controller to change the direction of the fly-through.

The participants were able to learn the fly-though features quickly and use them to easily navigate the colon. M.B. mentioned that a feature for varying the speed should be added to the system, as radiologists have varying reading preferences. While this feature is commonly used in the desktop setup, it is unclear what effects it would have in VR, and further studies on variable speed and locomotion need to be conducted.

Another observation by participants was made that it was more difficult to investigate areas on the bottom of the colon, which required the user to look down. In order to make it easier for the user to look down without causing nausea from the camera yaw rotation, we have added an additional rotation of the data. This interaction can be triggered by using the grip button and moving the wand. Once triggered, the user can change the roll of the data, thus bringing those "bottom" areas into the view of the user. Both of the participants have mentioned that having some sort of "floor" surface would be natural for navigation. We have added this feature in the form of a plane at the low end of the space (Figure 7). This "floor" surface acts as an additional frame of reference/cue during the rotation as it indicates that the colon data is being moved, and not the user. Furthermore, the intersection with the boundary of the colon helps to highlight the distance and scaling of the model in comparison to the height of the user, and gives them a visual cue similar to a glass floor when walking around the colon.

The complete stop in our system could be triggered with the use of any tool on the controller, but did not have a dedicated button. The participants have indicated that optional explicit controls would be useful as well, and that the "complete stop" button is "a must". We have followed these suggestions and have added the button. M.B. has suggested to also use the controller itself to control the direction of movement (antegrade and retrograde) and the speed of movement in a similar manner to the stick control of an aircraft.

Haptic feedback was suggested to be useful when backing up in order to prevent exiting the colon into empty space. Since users are mostly relying on automatic navigation along the centerline rather than locomotion for general navigation through the colon, they are not likely to exit the lumen of the colon, and this mechanism is mostly useful for closer investigation of an area by walking around within the colon. This haptic feedback was added after the study. We used the VRTK package [2] to estimate collision of the head position with the boundary of the colon mesh. When the user's head collides with the mesh, a haptic feedback with a strength of 4000 microseconds per frame is triggered, which is the maximum strength of vibration that the wand is capable of producing. This pulse is twice the strength of the aforementioned haptic feedback for interacting with widgets. Since visual cues of collision are observable upon forward navigation, based on our participants' feedback this haptic feedback is only applied when the user is walking backward into the colon wall (i.e., $\overrightarrow{v} \cdot \overrightarrow{n} > 0$, where $\overrightarrow{v}$ is the camera view direction and $\overrightarrow{n}$ is the surface normal at the collision point).

7.2.2 Measurement Mode

The experts noted that the 3D polyp measurement tool is easy to learn even though it was a novel approach for them to perform the measurement in 3D. Moreover, they have said that it is easier to fine tune the measurements in our 3D system than in the traditional desktop system. K.B. highlighted the ease of flying over the polyp to verify the measurement from multiple angles. Suggestions have included adding detail to the number of edits made (history), the potential accuracy of the measurement (based on automatic volumetric measurement), and the size of the ruler markers. We have addressed the last of these suggestions and have reduced the size of the ruler markers to ensure that they do not occlude the view of the area of measurement. It is important to note that for ease of navigation we maintained the collider region of the marker the same as in the original prototype.

7.2.3 Bookmark Mode

For the bookmarking tool, we have asked the experts whether they felt that the tool was sufficiently accurate to facilitate the picking of the approximate location of a polyp. They have noted that the accuracy of the tool was sufficient for placing the bookmark near the polyp and navigating to it later. The helpfulness of the directional ray indicating the end point of the ray was again underscored. The experts considered the process equivalent to the desktop counterpart and that it consumed an equivalent amount of time.

7.2.4 Flashlight Mode

The experts highlighted that even though a spotlight tool is available in some desktop software, such as Viatronix, the process of positioning the light is not intuitive. Since they do not have natural control, it is difficult to understand the depth that the light source is placed at and the exact direction. The IVC wand implementation solves this problem by offering a simple natural interface.

7.2.5 Electronic Biopsy Mode

The experts highlighted the electronic biopsy mode as the "single best feature of the system" and admired the feature of natural control over the beam size. At the time of the evaluation, the biopsy beam mode was available only during a complete stop. The experts have suggested extending the availability for the duration of the fly-through, and this feature has been added to our system after the evaluation session.

(a) (b)

Fig. 8. (a) Ileocecal valve as observed by the expert radiologists, using the electronic biopsy to highlight the difference between the valve and a polyp. (b) Experts experimenting with our IVC system.

7.2.6 Slice Viewing

In general diagnostic workflows, the slice view is the most essential, and is frequently the only view available to the radiologist. The slice stack is commonly navigated by scrolling, zooming into a specific location, and panning over the slice. In our first prototype, zooming and panning of the slice was missing, which was immediately noted by the experts. Afterward, we added a 2D focused zoom feature to the slice view, thus enabling the zoom on the targeted 2D area. For a VC application, the experts have suggested adding three standard viewing windows to start, which can later be extended to a full view window control with an established interaction mode. Alternating between a locally magnified view and the normal view of the slice enables the expert to observe the slice in both the context of the overall colon and the local area of interest. Moreover, the volumetric view with cutting plane was not well received by either of the domain experts. They both preferred to focus and navigate through the slices within individual windows. This feedback shows that the popular cutting plane technique was not preferred in this domain, even though it can be useful for exploring other medical data. We modified our final version, removing the volume view but retaining the small mesh view.

7.3 Limitations

The major limitations of our IVC system are the standard drawbacks inherent in HMDs, including cybersickness, the weight of the headset which must be worn, and being somewhat uncomfortable to use while standing. Additionally, the pixels per degree resolution of HMDs is currently much less than that of high resolution desktop monitors. However, VR headset technology is rapidly advancing, with reductions in weight, increased resolution, and improved latency.

Regarding functionality, we were able to address the main feedback from the radiologists, as discussed above. However, some of the open ended feedback could not be easily addressed. This included a method to adjust the windowing parameters for the CT slice views on the fly. Additionally, dynamic interaction with the surface of the colon to differentiate the softness of the tissue for better understanding of the surface was a requested feature. While such an interaction would make sense in a VR system, this will require further algorithm development and research into processing the CT Scans to determine tissue softness.

8 Conclusions and Future Work

We have presented a pipeline for immersive analysis in VC and an interaction paradigm for the elements of VC within VR. We received positive feedback from the experts on the natural interactions and the perceived faster fly-through. They found that both measurement and camera manipulation was easier than on the desktop VC, and the stereoscopic view helped with observing colon shape features while performing electronic biopsy. The task of delivering a VC system in VR faced performance challenges, which were solved by using an iso-surface mesh to improve rendering performance through space skipping throughout the volume rendering, lighting, and shadow calculations.

In the future, we plan to perform a formal study on the benefits of immersive analysis in VC. We also wish to port the interactions and visualization methods to other medical applications, along with improving the rendering for accelerated rendering of transparent volumes.

Acknowledgments

We thank Dr. Matthew Barish and Dr. Kevin Baker from the Radiology Department of Stony Brook University Hospital for evaluating our system and providing us with insightful feedback and suggestions. This work has been partially supported by National Science Foundation grants CNS-1302246, NRT-1633299, CNS-1650499.

References

[1] virtual tour fly camera. https://www.assetstore.unity3d.com/en/#!/content/56728. Accessed: 2017-09-30.

[2] VRTK - virtual reality toolkit. https://vrtoolkit.readme.io. Accessed: 2017-09-30.

[3] F. Argelaguet and C. Andujar. A survey of 3D object selection techniques for virtual environments. *Computers & Graphics*, 37(3):121–136, 2013.

[4] L. Besançon, P. Issartel, M. Ammi, and T. Isenberg. Usability comparison of mouse, touch and tangible inputs for 3D data manipulation. *arXiv preprint arXiv:1603.08735*, abs/1603.08735, 2016.

[5] L. Besançon, P. Issartel, M. Ammi, and T. Isenberg. Hybrid tactile/tangible interaction for 3D data exploration. *IEEE Trans. Vis. Comput. Graph.*, 23(1):881–890, 2017.

[6] S. Bhushan, S. Anandasabapathy, and R. Shukla. Use of augmented reality and virtual reality technologies in endoscopic training. *Clinical Gastroenterology and Hepatology*, 16(11):1688–1691, 2018.

[7] I. Bitter, A. E. Kaufman, and M. Sato. Penalized-distance volumetric skeleton algorithm. *IEEE Trans. Vis. Comput. Graph.*, 7(3):195–206, 2001.

[8] P. M. Boiselle, D. Levine, P. J. Horwich, L. Barbaras, D. Siegal, K. Shillue, and D. Affeln. Repetitive stress symptoms in radiology: Prevalence and response to ergonomic interventions. *J. Am. Coll. Radiol.*, 5(8):919–923.

[9] G. Bruder, F. Steinicke, and W. Stuerzlinger. Touching the void revisited: Analyses of touch behavior on and above tabletop surfaces. *Proc. of IFIP Human-Computer Interaction - INTERACT*, pages 278–296, 2013.

[10] K. N. Christensen, J. L. Fidler, J. G. Fletcher, R. MacCarty, and C. D. Johnson. Pictorial review of colonic polyp and mass distortion and recognition with the CT virtual dissection technique. *RadioGraphics*, 30(5):e42, 2010.

[11] D. Coffey, N. Malbraaten, T. B. Le, I. Borazjani, F. Sotiropoulos, A. G. Erdman, and D. F. Keefe. Interactive slice WIM: Navigating and interrogating volume data sets using a multisurface, multitouch VR interface. *IEEE Trans. Vis. Comput. Graph.*, 18(10):1614–1626, 2012.

[12] A. V. Dam, A. S. Forsberg, D. H. Laidlaw, J. J. LaViola, and R. M. Simpson. Immersive VR for scientific visualization: A progress report. *IEEE Comput. Graph. Appl.*, 20(6):26–52, 2000.

[13] J. E. East, B. P. Saunders, D. Boone, D. Burling, S. Halligan, and S. A. Taylor. Uni- and bidirectional wide angle CT colonography: effect on missed areas, surface visualization, viewing time and polyp conspicuity. *European Radiology*, 18(9):1910–1917, 2008.

[14] J. E. East, B. P. Saunders, D. Burling, D. Boone, S. Halligan, and S. A. Taylor. Surface visualization at CT colonography simulated colonoscopy: Effect of varying field of view and retrograde view. *The American Journal of Gastroenterology*, 102(11):2529–2535, 2007.

[15] J. L. Fidler, R. L. MacCarty, S. J. Swensen, J. E. Huprich, W. G. Thompson, T. L. Hoskin, and J. A. Levine. Feasibility of using a walking workstation during CT image interpretation. *J. Am. Coll. Radiol.*, 5(11):1130 – 1136, 2008.

[16] S. F. F. Gibson. Constrained elastic surface nets: Generating smooth surfaces from binary segmented data. *Proc. of MICCAI*, pages 888–898, 1998.

[17] W. N. Griffin, W. L. George, T. J. Griffin, J. G. Hagedorn, M. Olano, S. G. Satterfield, J. S. Sims, and J. E. Terrill. Application creation for an immersive virtual measurement and analysis laboratory. *Proc. of IEEE Workshop on Software Engineering and Architectures for Realtime Interactive Systems (SEARIS)*, pages 1–7, 2016.

[18] T. Grossman and R. Balakrishnan. The design and evaluation of selection techniques for 3D volumetric displays. *Proc. of ACM Symp. on User Interface Softw. and Technol. (UIST)*, pages 3–12, 2006.

[19] Y. Guiard. Asymmetric division of labor in human skilled bimanual action. *Journal of Motor Behavior*, 19(4):486–517, 1987.

[20] J. G. Hagedorn, J. P. Dunkers, S. G. Satterfield, A. P. Peskin, J. T. Kelso, and J. E. Terrill. Measurement tools for the immersive visualization environment: Steps toward the virtual laboratory. *J. Res. Natl. Inst. Stand. Technol.*, 112(5):257, 2007.

[21] A. Hann, B. M. Walter, N. Mehlhase, and A. Meining. Virtual reality in GI endoscopy: Intuitive zoom for improving diagnostics and training. *Gut*, 2018.

[22] E. Hoggan, S. A. Brewster, and J. Johnston. Investigating the effectiveness of tactile feedback for mobile touchscreens. *Proc. of SIGCHI Conf. Hum. Factor Comput. Syst.*, pages 1573–1582, 2008.

[23] L. Hong, S. Muraki, A. Kaufman, D. Bartz, and T. He. Virtual voyage: Interactive navigation in the human colon. *Proc. of SIGGRAPH*, pages 27–34, 1997.

[24] W. Hong, F. Qiu, and A. Kaufman. A pipeline for computer aided polyp detection. *IEEE Trans. Vis. Comput. Graph.*, 12(5):861–868, 2006.

[25] W. Hong, J. Wang, F. Qiu, A. Kaufman, and J. Anderson. Colonoscopy simulation. *Proc. of SPIE Medical Imaging*, 2007.

[26] T. Isenberg and M. Hancock. Gestures vs. postures: 'gestural' touch interaction in 3D environments. *Proc. of CHI Workshop on "The 3rd Dimension of CHI: Touching and Designing 3D User Interfaces" (3DCHI)*, pages 53–61, 2012.

[27] B. Jackson, B. Jelke, and G. Brown. Yea big, yea high: A 3D user interface for surface selection by progressive refinement in virtual environments. *Proc. of IEEE Virtual Reality*, pages 320–326, 2018.

[28] B. Jackson, T. Y. Lau, D. Schroeder, K. C. Toussaint Jr., and D. F. Keefe. A lightweight tangible 3D interface for interactive visualization of thin fiber structures. *IEEE Trans. Vis. Comput. Graph.*, 19(12):2802–2809, 2013.

[29] T. Klein, F. Guéniat, L. Pastur, F. Vernier, and T. Isenberg. A design study of direct-touch interaction for exploratory 3D scientific visualization. *Computer Graphics Forum*, 31(3pt3):1225–1234, 2012.

[30] B. Laha, D. A. Bowman, D. H. Laidlaw, and J. J. Socha. A classification of user tasks in visual analysis of volume data. *Proc. of IEEE Scientific Visualization*, pages 1–8, 2015.

[31] B. Laha, D. A. Bowman, and J. D. Schiffbauer. Validation of the MR simulation approach for evaluating the effects of immersion on visual analysis of volume data. *IEEE Trans. Vis. Comput. Graph.*, 19(4):529–538, 2013.

[32] B. Laha, K. Sensharma, J. D. Schiffbauer, and D. A. Bowman. Effects of immersion on visual analysis of volume data. *IEEE Trans. Vis. Comput. Graph.*, 18(4):597–606, 2012.

[33] S. Lee and G. J. Kim. Effects of haptic feedback, stereoscopy, and image resolution on performance and presence in remote navigation. *International Journal of Human-Computer Studies*, 66(10):701 – 717, 2008.

[34] W. Li, K. Mueller, and A. Kaufman. Empty space skipping and occlusion clipping for texture-based volume rendering. *Proc. of IEEE Visualization*, pages 317–324, 2003.

[35] D. López, L. Oehlberg, C. Doger, and T. Isenberg. Towards an understanding of mobile touch navigation in a stereoscopic viewing environment for 3D data exploration. *IEEE Trans. Vis. Comput. Graph.*, 22(5):1616–1629, 2016.

[36] C. Lundstrom, T. Rydell, C. Forsell, A. Persson, and A. Ynnerman. Multi-touch table system for medical visualization: Application to orthopedic surgery planning. *IEEE Trans. Vis. Comput. Graph.*, 17(12):1775–1784, 2011.

[37] J. Marino, W. Du, M. Barish, E. Li, W. Zhu, and A. Kaufman. Evaluation of electronic biopsy for clinical diagnosis in virtual colonoscopy. *Proc. of SPIE Medical Imaging*, 7964:796419–796419–8, 2011.

[38] M. R. Mine. Virtual environment interaction techniques. Technical report, 1995.

[39] K. Mirhosseini, Q. Sun, K. C. Gurijala, B. Laha, and A. E. Kaufman. Benefits of 3D immersion for virtual colonoscopy. *Proc. of IEEE VIS International Workshop on 3DVis*, pages 75–79, 2014.

[40] S. Mirhosseini, I. Gutenko, S. Ojal, J. Marino, and A. Kaufman. Automatic speed and direction control along constrained navigation paths. *Proc. of IEEE Virtual Reality*, pages 29–36, 2017.

[41] E. Monclús, J. Díaz, I. Navazo, and P.-P. Vázquez. The virtual magic lantern: An interaction metaphor for enhanced medical data inspection. *Proc. of ACM Symp. Virtual Real. Softw. Technol.*, pages 119–122, 2009.

[42] E. Monclús, P.-P. Vázquez, and I. Navazo. Data-aware picking for medical models. *Proc. of International Conference on Computer Vision, Imaging and Computer Graphics*, pages 50–65, 2013.

[43] S. Nadeem, J. Marino, X. Gu, and A. Kaufman. Corresponding supine and prone colon visualization using eigenfunction analysis and fold modeling. *IEEE Trans. Vis. Comput. Graph.*, 23(1):751–760, 2017.

[44] D. Pamungkas and K. Ward. Electro-tactile feedback system to enhance virtual reality experience. *Int. J. Comput. Assist. Radiol. Surg.*, 8(6):465, 2016.

[45] V. M. Pawar and A. Steed. Profiling the behaviour of 3D selection tasks on movement time when using natural haptic pointing gestures. *Proc. of ACM Symp. Virtual Real. Softw. Technol.*, pages 79–82, 2009.

[46] P. J. Pickhardt, J. R. Choi, I. Hwang, J. A. Butler, M. L. Puckett, H. A. Hildebrandt, R. K. Wong, P. A. Nugent, P. A. Mysliwiec, and W. R. Schindler. Computed tomographic virtual colonoscopy to screen for colorectal neoplasia in asymptomatic adults. *New England Journal of Medicine*, 349(23):2191–2200, 2003.

[47] P. J. Pickhardt and D. H. Kim. CT colonography. *Radiologic Clinics*, 51(1):69–88, 2017.

[48] B. J. Pollard, E. Samei, A. S. Chawla, C. Beam, L. E. Heyneman, L. M. H. Koweek, S. Martinez-Jimenez, L. Washington, N. Hashimoto, and H. P. McAdams. The effects of ambient lighting in chest radiology reading rooms. *Journal of Digital Imaging*, 25(4):520–526, 2012.

[49] B. Preim, C. Tietjen, W. Spindler, and H. O. Peitgen. Integration of measurement tools in medical 3D visualizations. *Proc. of IEEE Visualization*, pages 21–28, 2002.

[50] E. D. Ragan, R. Kopper, P. Schuchardt, and D. A. Bowman. Studying the effects of stereo, head tracking, and field of regard on a small-scale spatial judgment task. *IEEE Trans. Vis. Comput. Graph.*, 19(5):886–896, 2013.

[51] B. Reitinger, D. Schmalstieg, A. Bornik, and R. Beichel. Spatial analysis tools for virtual reality-based surgical planning. *Proc. of IEEE Symp. 3D User Interfaces*, pages 37–44, 2006.

[52] I. Rössling, C. Cyrus, L. Dornheim, A. Boehm, and B. Preim. Fast and flexible distance measures for treatment planning. *Int. J. Comput. Assist. Radiol. Surg.*, 5(6):633–646, 2010.

[53] M. Rowan and P. Kenny. Determining appropriate ambient lighting levels in radiology reporting rooms. *Physica Medica: European Journal of Medical Physics*, 30(6):722, 2014.

[54] L. Ruess, S. C. O'Connor, K. H. Cho, F. H. Hussain, W. J. Howard, R. C. Slaughter, and A. Hedge. Carpal tunnel syndrome and cubital tunnel syndrome: Work-related musculoskeletal disorders in four symptomatic radiologists. *American Journal of Roentgenology*, 181(1):37–42, 2003.

[55] D. Schmalstieg, L. M. Encarnação, and Z. Szalavári. Using transparent props for interaction with the virtual table. *Proc. of ACM SIGGRAPH Symp. Interact. 3D Graph. Games*, pages 147–153, 1999.

[56] U. Schultheis, J. Jerald, F. Toledo, A. Yoganandan, and P. Mlyniec. Comparison of a two-handed interface to a wand interface and a mouse interface for fundamental 3D tasks. *Proc. of IEEE Symp. 3D User Interfaces*, pages 117–124, 2012.

[57] P.-P. Sloan, J. Kautz, and J. Snyder. Precomputed radiance transfer for real-time rendering in dynamic, low-frequency lighting environments. *ACM Trans. Graph.*, 21(3):527–536, 2002.

[58] P. Song, W. B. Goh, C.-W. Fu, Q. Meng, and P.-A. Heng. WYSIWYF: exploring and annotating volume data with a tangible handheld device. *Proc. of SIGCHI Conf. Hum. Factor Comput. Syst.*, pages 1333–1342, 2011.

[59] M. Van Beurden, W. IJsselsteijn, and J. Juola. Effectiveness of stereoscopic displays in medicine: a review. *3D Research*, 3(1):3, 2012.

[60] R. L. Van Uitert and R. M. Summers. Automatic correction of level set based subvoxel precise centerlines for virtual colonoscopy using the colon outer wall. *IEEE Trans. Med. Imaging*, 26(8):1069–1078, 2007.

[61] M. Wan, Z. Liang, Q. Ke, L. Hong, I. Bitter, and A. Kaufman. Automatic centerline extraction for virtual colonoscopy. *IEEE Trans. Med. Imaging*, 21(12):1450–1460, 2002.

[62] Z. Wang, Z. Liang, L. Li, B. Li, D. Eremina, and H. Lu. An improved electronic colon cleansing method for detection of colonic polyps by virtual colonoscopy. *IEEE Trans. on Biomed. Eng.*, 53(8):1635–46, 2006.

[63] T. Wen, D. Medveczky, J. Wu, and J. Wu. Colonoscopy procedure simulation: Virtual reality training based on a real time computational approach. *BioMedical Engineering OnLine*, 17(1):9, 2018.

[64] S. You, L. Hong, M. Wan, K. Junyaprasert, A. Kaufman, S. Muraki, Y. Zhou, M. Wax, and Z. Liang. Interactive volume rendering for virtual colonoscopy. *Proc. of IEEE Visualization*, pages 433–436, 1997.

[65] E. J. Yun, C. S. Choi, D. Y. Yoon, Y. L. Seo, S. K. Chang, J. S. Kim, and J. Y. Woo. Combination of magnetic resonance cholangiopancreatography and computed tomography for preoperative diagnosis of the mirizzi syndrome. *Journal of Computer Assisted Tomography*, 33(4), 2009.

[66] W. Zeng, J. Marino, K. C. Gurijala, X. Gu, and A. Kaufman. Supine and prone colon registration using quasi-conformal mapping. *IEEE Trans. Vis. Comput. Graph.*, 16(6):1348–1357, 2010.